https://doi.org/10.5755/j02.eie.38283

ELEKTRONIKA IR ELEKTROTECHNIKA, ISSN 1392-1215, VOL. 30, NO. 5, 2024

Modelling Solar Irradiance Data for Energy Harvesting IoT Sensors

Jan Choutka, Jiri Konecny, Miroslav Mikus, Kamil Bancik, Michal Prauzek, Jaromir Konecny*

Department of Cybernetics and Biomedical Engineering, VSB - Technical University of Ostrava,
17. listopadu 2172/15, 708 00 Ostrava-Poruba, Czech Republic
jan.choutka@vsb.cz; jiri.konecny@vsb.cz; miroslav.mikus@vsb.cz; kamil.bancik@vsb.cz; michal.prauzek@vsb.cz;
**jaromir.konecny@vsb.cz*

***Abstract*—Managing energy in batteryless Internet of Things (IoT) nodes, especially in solar-powered mesh networks, presents significant challenges. This paper introduces an advanced solar irradiance model that simulates detailed daily energy profiles. The model considers various azimuth and elevation angles of solar panels, as well as cloud cover. Accurate simulation of daily energy production is critical for optimising the behaviour of solar-powered IoT nodes. The results highlight the utility of the model as a robust tool for research and simulations involving batteryless IoT devices, emphasising its enhanced capabilities for precise energy management and optimisation. This study offers a reliable framework for predicting and managing energy production in solar-powered IoT networks, thus supporting the development of more efficient and sustainable IoT systems.**

***Index Terms*—Solar model; Energy management; Internet of Things.**

I. INTRODUCTION

The use of remote sensing monitoring systems is currently experiencing a surge in popularity due to its advantages in remote and challenging locations. These systems are being actively deployed for monitoring and remote sensing operations, functioning both as early warning systems (EWS) [1] and integral components of the Internet of Things (IoT) [2]. Additionally, they serve a wide range of applications, including environmental surveillance [3], precision agriculture [4], and infrastructure management. The low accessibility and challenging conditions in areas where sensor networks are deployed have created a strong demand for the development of resilient and reliable maintenance-free devices [5]. Current battery technology requires frequent replacement, incurs high operational costs, exhibits sensitivity to temperature variations, and lacks ecological sustainability. A potential solution to these drawbacks is energy harvesting. However, unlike batteries, energy harvesting yields an inconsistent, fluctuating supply of energy [6]. Therefore, researchers are increasingly exploring intelligent energy management solutions. To develop an intelligent energy management system, it is important to create simulations of the environments in which these systems will operate [7]. Meteorological stations are typically located near these systems and are a convenient means of collecting the relevant data for predicting energy supplies and setting up energy harvesting devices. Nevertheless, minor disparities in device placement and characteristics require that all variations be tested in a system model.

The paper introduces a model that decomposes historical solar irradiance data, including the total irradiance as a sum of direct and diffuse components, into its individual direct and diffuse components. This decomposition is essential because many meteorological stations and solar power plants provide only the total irradiance data, making it necessary to separate these components using known factors such as position and date.

These decomposed values are subsequently used in simulations of solar panels positioned in various orientations. This is crucial for simulating batteryless IoT nodes, which are placed at different azimuths and elevations and therefore receive inconsistent energy inputs. Simulating these conditions helps estimate the energy harvested for each node.

Figure 1 illustrates the system model. Historical data are decomposed into direct and diffuse components and then input into a solar panel model implemented in Matlab code. This model simulates the energy intake for panels orientated in different directions. The output is the estimated harvested energy, which is used to simulate a mist computing IoT node network. This simulation can account for various weather conditions, such as multiday storms, and their impact on the energy supply to the nodes.

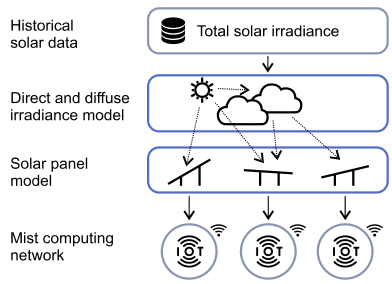

Fig. 1 Historical data for total solar irradiance are processed in a model that decomposes solar irradiance into direct and diffuse components. The solar panel model subsequently estimates the available energy via a mist computing network.

Manuscript received 24 May, 2024; accepted 30 August, 2024.

This article has been produced with the financial support of the European Union under the REFRESH – Research Excellence for REgion Sustainability and High-tech Industries project under Grant No. CZ.10.03.01/00/22_003/0000048 via the Operational Programme Just Transition. This work was supported by the project "Development of algorithms and systems for control, measurement and safety applications X" of Student Grant System under Grant No. SP2024/021, VSB-TU Ostrava.

The sensor network determines the energy available in the nearby environment using data from a single weather station [8]. In addition to assessing current energy availability, it is crucial to forecast future energy availability based on meteorological conditions. Predicting this parameter allows sensor nodes to effectively plan their operational modes and optimise energy consumption according to forecast weather changes. The present study contributes the following.

– A mathematical model proposed that estimates the energy obtained from groups of small solar panels with various orientations.

– A simulation of the effect of clouds on the proposed model under various weather conditions.

– Model validation with real data: Testing and validation of the accuracy of the model using historical data from solar panels and meteorological stations.

– Suggestion of implementation in IoT networks: Integration of the model into IoT node networks to ensure reliable and efficient operation of sensor networks in real time.

The rest of this article is organised as follows. Section II presents related works. Section III provides a description of the proposed model and methods. Section IV provides a detailed description of the results, and Section V discusses the results in the context of state-of-the-art methods, highlighting the significance of the study and its limitations. Finally, Section VI concludes the article.

II. Related Works

In this section, the focus is on describing works related to this and highlighting the differences between them. Existing methods and technologies in the field of solar modelling are analysed, discussing both their strengths and weaknesses. The identified shortcomings of these approaches are addressed by the proposed solution, which brings new perspectives and improvements to the area of solar irradiance modelling.

Table I shows an overview of the state-of-the-art methods that provide solar models. A comprehensive review of these solar models is described in [9]. The authors use various models and compare them at different locations in China. However, all of the models presented are capable of modelling horizontal panels only.

TABLE I. TABLE OF SOURCES OF SELECTED APPROACHES FOR MEASURING AND CALCULATING SOLAR IRRADIANCE UNDER THE EFFECT OF VARIOUS ATMOSPHERIC CONDITIONS.

Authors	Topic	Data	Cloud model	Results	Limits
Cai, Qin, Wang, Hu, and Zhang [9]	The authors created a MATLAB library containing several methods for calculating irradiance	Hourly solar irradiance was measured hourly at 35 stations across China	Modelled with a machine learning algorithm	Machine learning models	Absence of a relevant input parameter
Hottel [10]	The study proposes constants for four climates to calculate solar radiation as a simple equation	Data used for comparative purposes were measured with a pyranometer	Not calculated	Constants for calculating clear-sky conditions at various altitudes and climates were introduced into the model, yielding measurements with 0.3 %	This method does not calculate with cloud effects
Kambezidis, Mimidis, and Kavadias [11]	The authors examine the variations in clear-sky conditions throughout the year, considering different rotations of solar panels but not changes in the solar beam itself	Data were collected from 43 meteorological stations across southeastern Europe	Values measured at 43 meteorological stations were applied	Formulas were developed to estimate the solar energy potential at any location in Greece, using the available data	Information about clouds must be measured at meteorological station
Ruiz-Arias [12]	The authors apply filters that represent suspended aerosols in the air, representing the formation of clouds with varying shape and density	Ground stations, including 15 years of direct normal irradiance measurements	Clouds were modelled as series of filters	10 % for diffuse irradiation, 2 % for direct irradiation (standard deviation error)	Absence of a relevant input parameter
Dazhi, Jirutitijaroen, and Walsh [13]	The authors suggested three models to predict next-hour solar irradiance	Two meteorological stations from USA in Miami and Orlando	Weather index based on regression analysis to predict cloud transients and a look-up table for irradiance	Models capable of predicting next-hour solar irradiance based on current data	Cannot be calculated with panel angle
Diez, Martínez-Rodríguez, Navas-Gracia, Chico-Santamarta, Correa-Guimaraes, and Andara [14]	Modelling solar radiation on tilted PV panels	Horizontal global solar irradiation hours from nearby meteorological station	Anisotropic models of diffuse solar irradiation	Improved estimations of solar irradiation on the inclined plane using anisotropic models, with RMSE values as low as 11.95 W/m² and R^2 values up to 0.9835 for different models and days	The model requires pyranometer data as input information
Furlan, de Oliveira, Soares, Codato, and Escobedo [15]	The study introduces a new regression model to estimate hourly values of	Hourly values of global and diffuse solar radiation, air	Modelled with a regression algorithm that	Coefficient of determination R^2 of 0.93	Visual observation of clouds can introduce errors,

Authors	Topic	Data	Cloud model	Results	Limits
	diffuse solar radiation at the surface, incorporating cloud effects	temperature, relative humidity, atmospheric pressure, cloudiness, cloud type, and particulate matter measured in São Paulo, Brazil, during the year 2002	includes the effects of cloudiness, cloud type, and traditional meteorological variables		limited temporal resolution, and spatial representativeness of the cloud data. These data cannot be received from all meteorological stations

Solar irradiation can be calculated using a physical model that includes air mass modelling [10]. However, clouds must also be considered, which significantly affect the resulting solar irradiance values on the Earth's surface. Advanced models that incorporate the effect of cloud cover and are capable of modelling various panel elevations and azimuths typically rely on advanced historical data or historical data from many weather stations [11].

Another approach to modelling solar radiance is the use of filters. Solar irradiance is modelled as a series of mathematical filters [12]. The advantage of this approach is the complex model of solar irradiance; however, it requires advanced historical data to be measured.

The authors in [13] explore the prediction of solar irradiance for the next hour using three different methods. They utilise meteorological data, including three types of irradiances and cloud cover, employing auto-regressive integrated moving average (ARIMA) models. All three methods were tested using data from meteorological stations in Miami and Orlando, demonstrating that incorporating cloud cover information improves forecast accuracy.

The authors in [14] have thus attempted to estimate the hourly global solar irradiance on tilted and orientated photovoltaic solar panels applied to greenhouse production. They used horizontal solar irradiance data from agrometeorological stations and anisotropic diffuse solar irradiance models to improve estimates of solar irradiance on a tilted surface.

The authors in [15] seek to develop a new regression model to estimate hourly values of diffuse solar radiation from the surface that incorporate the effects of clouds, traditional meteorological variables, and air pollution to improve the accuracy of the predictions of this radiation.

III. MODEL AND METHODS

This paper introduces a mathematical model capable of simulating the solar beam, diffuse radiation, clouds, and air mass. Additionally, the model can simulate a solar panel with variable zenith and azimuth angles.

Figure 2 shows a block diagram of a model designed to calculate the power output of a solar panel. The model extends the calculation of solar energy with the calculation of an equivalent area and cloud simulations. The first step in calculating solar irradiance involves determining the direction of solar radiation based on the Earth's position and the current time. The calculation is performed by the Solar Beam block, which outputs the azimuth and elevation of the solar panel array. As solar radiation passes through the atmosphere, it loses a certain amount of energy, which is calculated by an Air Mass block. Direct solar radiation strikes the solar panel at a certain angle, necessitating the calculation of an equivalent area. The total solar irradiance is then calculated by summing the diffuse radiation and direct radiation. In addition, solar irradiance is adjusted by a cloud coefficient to account for cloud cover. The resultant power obtained from a particular solar panel is calculated according to the size and efficiency of the panel.

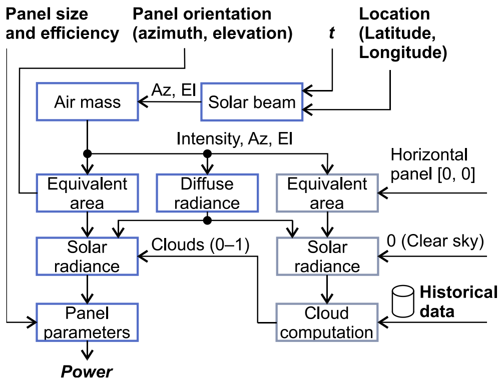

Fig. 2. Block diagram illustrating a model capable of calculating the power output of a solar panel.

To incorporate the impact of clouds into the model, a cloud simulator was added. The cloud data were obtained from a historical data set containing global irradiance values. The real global irradiance is compared to the simulated global irradiance without clouds. The simulated global irradiance was derived from the model with the solar panel positioned horizontally (elevation is zero).

Calculation of the azimuth and altitude of the solar beam is described in [16]. The solar beam is represented as a vector in three-dimensional space, pointing to the ground. The angle of the solar beam is calculated for each time interval.

As the solar beam permeates the atmosphere, it loses energy due to refraction and heats the air molecules within the air mass. The air mass index represents the amount of material through which the beam passes. A beam perpendicular to the surface has an index of 1, while a beam parallel to the ground surface has an infinite index. The air mass calculation is defined as follows [17]:

$$\varphi = 90 - El_s, \tag{1}$$

$$AM = \frac{1}{\cos(\varphi) + 0.50572 \cdot (96.07995 - \varphi)^{-1.6364}}, \tag{2}$$

$$c_1 = 1.135, \tag{3}$$

$$c_2 = 0.678, \tag{4}$$

$$\text{Intensity} = c_1 \cdot 0.7^{AM^{c_2}} \ (\text{W}), \tag{5}$$

where AM is the air mass index, with a value of 1 representing a perpendicular angle to the ground, El_s represents the solar elevation, and Intensity is the power of the solar beam. The vector of the solar beam is obtained by combining the

Intensity with azimuth and elevation.

The solar beam intensity vector strikes the solar panel at a certain angle; therefore, the equivalent area of the solar panel is calculated as follows:

$$h_x = \sin\left(\pi/2 - El_p\right)\cdot\cos\left(\pi/2 + Az_p\right), \quad (6)$$

$$h_y = \sin\left(\pi/2 - El_p\right)\cdot\cos\left(\pi/2 + Az_p\right) \quad (7)$$

$$h_z = \cos\left(\pi/2 - El_p\right), \quad (8)$$

$$\overrightarrow{h_{vec}} = \left(h_x, h_y, h_z\right), \quad (9)$$

$$\overrightarrow{w_{vec}} = \left(\cos\left(Az_p\right), \sin\left(Az_p\right), 0\right), \quad (10)$$

$$S_{eq} = \left(\overrightarrow{w_{vec}} \times \overrightarrow{h_{vec}}\right)\cdot\left(\overrightarrow{\varphi_s}\right)^T, \quad (11)$$

where S_{eq} is the area of the solar panel perpendicular to sunlight that would generate the same energy as a tilted solar panel with an area of one, El_p is the panel elevation angle, Az_p is the panel azimuth angle, and φ is the normalised vector of the solar beam striking the surface of the solar panel.

The diffuse irradiance depends on various factors. It comprises terrestrial radiation, which is energy reflected from the ground, hills, and nearby objects, and scattered solar radiation is the energy redirected to solar panels by clouds. Because modelling these factors is complex, a constant value of IR = 10 % of direct irradiance can be applied to approximate these minor irradiance contributions.

To determine the amount of sunlight blocked by clouds, the proposed model uses historical data collected from weather stations. The approach involves simulating clear-sky conditions at a specific location, mirroring the geographical context of the historical data, and subsequently comparing the simulated clear-sky scenario with historical observations. Cloud coverage is quantified as the ratio between historical and simulated values, expressed as

$$C_{\text{coef}} = 1 - \frac{\text{SR}_{\text{hist}}}{\text{SR}_{\text{sim,CS}}}, \quad (12)$$

where C_{coef} is the cloud coefficient, SR_{hist} denotes the historical solar irradiance value, and $\text{SR}_{\text{sim,CS}}$ is the simulated solar irradiance value under clear-sky conditions. In instances where the historical data align precisely with the simulated data, the cloud coefficient equals zero, indicating the absence of clouds.

Finally, the total solar irradiance is computed as follows

$$\text{SR}_{\text{sim}} = \\ = \left(\text{Intensity}\cdot S_{eq} + \text{IR}\cdot\text{Intensity}\right)\cdot\left(1 - C_{\text{coef}}\right)\left(\text{W}\right), \quad (13)$$

where SR_{sim} represents simulated solar power in Watts, Intensity denotes solar beam power after air mass correction, S_{eq} is the equivalent area, IR is the indirect irradiance coefficient, and C_{coef} is the cloud coefficient.

The model was implemented in MATLAB and its source code is available on GitHub [18] for reference and further exploration. The experiment was carried out to assess the effectiveness of the model in simulating the capture of solar radiation under diverse conditions. For this purpose, solar irradiance data from the Mošnov meteorological station (49.6918 ° latitude, 18.1126 ° longitude, altitude 252.8 metres) recorded at 10-minute intervals were used.

IV. Results

The presented model was tested with data for the months of March, June, September, and December to cover seasonal variations in solar irradiance. The solar panels were positioned at elevations of 30, 60, and 90 degrees and azimuths of 0 (North), 45, 90 (East), 135, 180 (South), 225, 270 (West), and 315 degrees. Each configuration was tested under clear and cloudy sky conditions to evaluate the model's responsiveness to atmospheric changes. The results include total 30-day cumulative energy obtained for a 1 cm^2 panel with an efficiency of 21 %. Additionally, the results present the total monthly total energy and illustrate daylight graphs for various panel orientations.

Table II presents the 30-day energy totals for a 1 cm^2 solar panel with a 21 % efficiency in different orientations under clear-sky conditions at the Mošnov location in 2016. The table includes monthly totals for March, June, September, and December to represent all four seasons. The energy totals are computed for clear-sky conditions, indicating that the results depict the theoretical maximum energy obtainable from the solar panel.

To emulate real-world conditions with more accuracy, cloud data from a historical data set were integrated into the model. Table III presents the 30-day energy totals for a 1 cm^2 solar panel with 21 % efficiency in various orientations under cloudy conditions at the Mošnov location in 2016. In general, the energy totals exhibit a significant reduction, with only 54 % of the total potential energy being obtained.

TABLE II. TOTAL ENERGY OVER 30 DAYS FOR A 1 CM^2 SOLAR PANEL WITH AN EFFICIENCY OF 21 %, IN VARIOUS ORIENTATIONS UNDER CLEAR-SKY CONDITIONS AT THE MOŠNOV LOCATION IN 2016.

Az. (→)	**El. (↓)**	**0 (N)**	**45**	**90 (E)**	**135**	**180 (S)**	**225**	**270 (W)**	**315**
March	30	1,92	2,95	4,66	6,13	6,66	5,91	4,41	2,79
	60	0,83	1,90	4,12	6,14	6,93	5,83	3,78	1,70
	90	0,83	1,46	3,22	4,88	5,57	4,57	2,87	1,28
June	30	10,88	11,29	12,72	13,73	14,03	13,91	12,93	11,40
	60	5,32	7,45	10,26	11,18	11,07	11,48	10,55	7,58
	90	3,00	5,15	7,30	7,14	6,04	7,40	7,45	5,10
September	30	4,26	5,71	8,36	10,52	11,32	10,32	8,11	5,55
	60	1,50	3,72	7,31	10,18	11,22	9,88	6,98	3,53
	90	1,45	2,80	5,64	7,84	8,51	7,54	5,30	2,61
December	30	0,46	0,53	1,54	2,83	3,39	2,79	1,49	0,53
	60	0,46	0,47	1,50	3,49	4,47	3,42	1,43	0,47
	90	0,46	0,46	1,30	3,34	4,47	3,26	1,24	0,46

TABLE. III. TOTAL ENERGY FOR 30 DAYS FOR A 1 CM^2 SOLAR PANEL WITH AN EFFICIENCY OF 21 %, IN VARIOUS ORIENTATIONS UNDER CLOUDY CONDITIONS AT THE MOŠNOV LOCATION IN 2016.

Az. (→)	El. (↓)	0 (N)	45	90 (E)	135	180 (S)	225	270 (W)	315
March	30	1,92	2,95	4,66	6,13	6,66	5,91	4,41	2,79
	60	0,83	1,90	4,12	6,14	6,93	5,83	3,78	1,70
	90	0,83	1,46	3,22	4,88	5,57	4,57	2,87	1,28
June	30	10,88	11,29	12,72	13,73	14,03	13,91	12,93	11,40
	60	5,32	7,45	10,26	11,18	11,07	11,48	10,55	7,58
	90	3,00	5,15	7,30	7,14	6,04	7,40	7,45	5,10
September	30	4,26	5,71	8,36	10,52	11,32	10,32	8,11	5,55
	60	1,50	3,72	7,31	10,18	11,22	9,88	6,98	3,53
	90	1,45	2,80	5,64	7,84	8,51	7,54	5,30	2,61
December	30	0,46	0,53	1,54	2,83	3,39	2,79	1,49	0,53
	60	0,46	0,47	1,50	3,49	4,47	3,42	1,43	0,47
	90	0,46	0,46	1,30	3,34	4,47	3,26	1,24	0,46

As expected, the tables present typical behaviour, indicating that the highest energy gain can be achieved during summer (June) when the solar panel is orientated south with an elevation of 30 degrees, which closely approximates the optimal elevation of 35 degrees for the Czech Republic. The results also confirm the well-established principle that a higher panel elevation can increase potential gains during winter, while gains during summer are limited, therefore, requiring a trade-off.

Figure 3 presents a bar graph illustrating the monthly income from solar energy for a 1 cm^2 solar panel with 21 % efficiency, orientated at 180 ° and elevated at 30 ° in Mošnov 2016. The blue bars indicate the energy income under clear-sky conditions, whereas the orange bars depict the energy income under cloudy conditions.

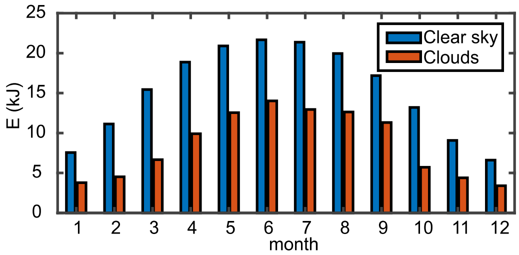

Fig. 3. Bar graph of the monthly incoming solar energy on a 1 cm^2 solar panel with an efficiency of 21 %, orientated 180 ° and elevated 30 °, in Mošnov 2016.

The primary aim of the proposed solution is to simulate the temporal behaviour of solar radiation rather than relying on statistical parameters. Essentially, the model is capable of computing solar irradiance for any given time and over any period. However, the incorporation of cloud cover data into the model requires historical data. For the present study, historical data with a 10-minute period were employed, enabling the model to simulate temporal behaviour at the same interval. It is important to note that meteorological stations typically provide data on global irradiance, which assumes a horizontally placed solar panel. Consequently, these data cannot be applied to panels with varying orientations and elevations.

Figure 4 illustrates the solar irradiance available for a panel with various azimuth angles at a fixed elevation of 30 ° on different types of days. Figures 4(a)–(d) present the solar irradiance patterns over time for different weather conditions.

Figure 4(a) shows the solar irradiance on a sunny summer day. Solar irradiance peaks around midday, with the highest values observed for an azimuth angle of 180 °. The maximum recorded irradiance is approximately 1000 W/m^2. Figure 4(b) represents a cloudy winter day. The irradiance values are significantly lower compared to a summer day, peaking at approximately 600 W/m^2. Fluctuations throughout the day indicate intermittent cloud cover. Figure 4(c) depicts spring conditions with rapid weather changes. Solar irradiance varies significantly, with sharp peaks and troughs throughout the day. The maximum irradiance reaches approximately 1000 W/m^2 during brief periods of clear sky. Figure 4(d) depicts the solar irradiance on a cloudy spring day. Similarly to a cloudy winter day, solar irradiance is lower, with peaks at approximately 600 W/m^2. Multiple peaks throughout the day correspond to intermittent clear periods.

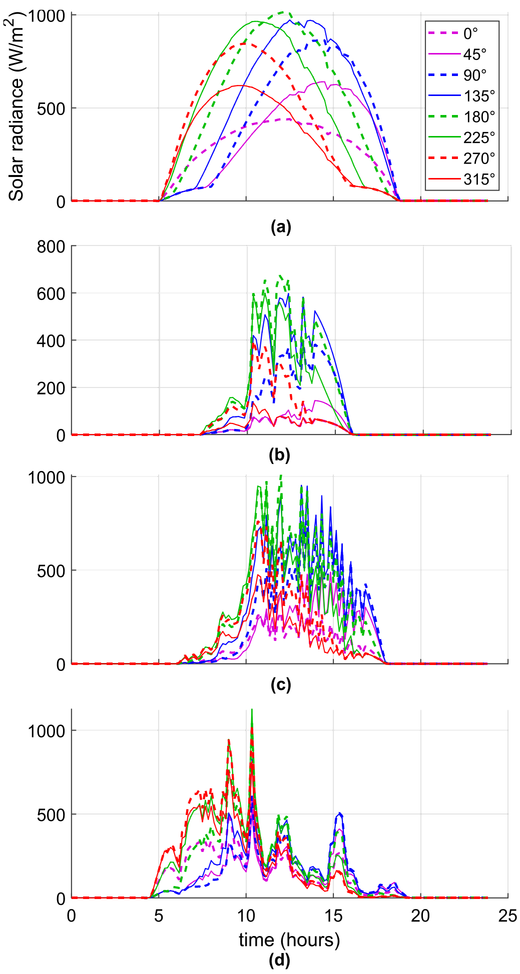

Fig. 4. Graph of solar irradiance in the panel for various azimuths and elevation of 30 ° under a range of weather and climate conditions: (a) Sunny summer day; (b) Cloudy winter day; (c) Spring with rapid weather changes; (d) Cloudy spring day.

V. Discussion

This section compares the proposed model with state-of-the-art methods and discusses its significance and limitations in the context of its novelty and contribution to the field.

Table IV compares the features of the proposed solution with state-of-the-art methods. Hottel’s model [10] is a widely applied physical model known for its robustness. However, it lacks the capability to account for diffuse radiation and does not allow for changes in panel orientation. On the contrary, the advanced physical model developed by Kambezidis, Mimidis, and Kavadias [11] integrates data from multiple stations, providing a comprehensive view of solar radiation. Nevertheless, this model provides only summary values and cannot capture detailed daily variations. Ruiz-Arias [12] propose a model that employs filters to simulate solar radiation. Although this approach can yield accurate results, it relies on complex historical data and cannot accommodate different panel orientations.

On the contrary, the solution proposed in the present study offers several distinct advantages. First, it incorporates both direct and diffuse radiation, providing a more comprehensive model of solar energy capture. Additionally, the proposed solution allows for the adjustment of panel orientation and elevation, allowing energy capture to be optimised according to specific site conditions. The model also simulates cloud coverage using historical solar irradiance data, incorporating the effect of these atmospheric conditions on solar energy capture in the solar panel array. Detailed daily profiles of solar radiation are also produced, which enhances the accuracy of the simulations and shows the versatility of the model as a tool for simulating solar energy capture.

TABLE. IV. COMPARISON OF THE PROPOSED SOLUTION’S FEATURES WITH STATE-OF-THE-ART METHODS.

Ref. No.	Model	Parameters	Direct	Diffuse	Panel or.	Clouds	Detailed Values
[4]	Physical	Cloud measurement	✔	✗	✗	✔	✔
[5]	Physical	Hist. data various locations	✔	✔	✔	✔	✗
[11]	Filters	Advance parameters	✔	✔	✗	✔	✔
[13]	Physical	Cloud cover of dome	✔	✔	✗	✔	✔
[14]	Physical	Three types of cloudiness	✔	✔	✔	✔	✔
[15]	Physical	Visual observation of clouds	✔	✔	✗	✔	✔
Proposed solution	Physical + Hist. data	Hist. data	✔	✔	✔	✔	✔

The significance of this study is in its development of a model that accurately simulates energy capture dynamics throughout the day. By integrating cloud simulation capabilities and using real data from a weather station, the model achieves improved reliability and applicability in real-world scenarios. The model is especially relevant for future research and simulations in connection with batteryless IoT devices. Its practical utility lies in its ability to predict and optimise energy harvesting processes.

The performance evaluation of the proposed model indicates a strong alignment between its predictions and the actual daily energy production patterns, demonstrating its accuracy and effectiveness. Unlike previous studies, the proposed model successfully integrates the ability of tilting solar panels, providing an effective solution for various applications. However, it is important to acknowledge the limitations of this approach. Simulation of diffuse radiation is based on a fixed percentage, which may not accurately reflect variations in meteorological conditions, e.g., during thunderstorms. This aspect requires further refinement to improve the accuracy of the model in a broader range of weather scenarios.

VI. Conclusions

In this study, we introduce a novel solar irradiance model specifically tailored to the energy management systems of batteryless Internet of Things (IoT) devices. The model effectively decomposes historical solar irradiance data into direct and diffuse components, simulates various solar panel orientations, and incorporates the impact of cloud cover. The validation of the model using data from the Mošnov meteorological station demonstrates its robustness and accuracy across different seasons and weather conditions. The results of the study highlight the utility of the model in predicting solar energy capture with high precision, which is a crucial factor in optimising the performance of solar-powered IoT networks. This capability enables better planning and energy management for devices in such networks. The model is therefore a valuable tool for the design of maintenance-free, resilient IoT devices for deployment in remote and inaccessible areas.

Compared to existing state-of-the-art methods, the proposed model is distinguished by several key features. Specifically, the model provides detailed daily energy profiles, accommodates variable solar panel orientations, and accurately simulates the effects of clouds on the ability of a solar panel to capture solar energy. While the model’s reliance on historical data for cloud simulation limits its predictive accuracy in unprecedented weather scenarios, future enhancements could address this by integrating real-time meteorological data and advanced weather prediction algorithms.

In conclusion, the proposed solar irradiance model offers a comprehensive and practical approach to energy harvesting for batteryless IoT devices. The model lays the foundation for more efficient and sustainable IoT solutions. The continued refinement and application of the model has the potential to significantly contribute to advancements in energy management strategies for IoT networks. By providing accurate predictions of solar energy availability, the model holds promise for various fields, including environmental monitoring, precision agriculture, and infrastructure management, and can support the widespread adoption of solutions that employ renewable energy.

CONFLICTS OF INTEREST

The authors declare that they have no conflicts of interest.

REFERENCES

[1] M. Esposito, L. Palma, A. Belli, L. Sabbatini, and P. Pierleoni, "Recent advances in Internet of Things solutions for early warning systems: A review", *Sensors*, vol. 22, no. 6, p. 2124, 2022. DOI: 10.3390/s22062124.

[2] C. Du and S. Zhu, "Research on urban public safety emergency management early warning system based on technologies for the Internet of Things", *Procedia Engineering*, vol. 45, pp. 748–754, 2012. DOI: 10.1016/j.proeng.2012.08.234.

[3] S. Sadowski and P. Spachos, "Wireless technologies for smart agricultural monitoring using internet of things devices with energy harvesting capabilities", *Computers and Electronics in Agriculture*, vol. 172, art.105338, 2020. DOI: 10.1016/j.compag.2020.105338.

[4] M. Saxena and S. Dutta, "Improved the efficiency of IoT in agriculture by introduction optimum energy harvesting in WSN", in *Proc. of 2020 International Conference on Innovative Trends in Information Technology (ICITIIT)*, 2020, pp. 1–5. DOI: 10.1109/ICITIIT49094.2020.9071549.

[5] S. Khernane, S. Bouam, and C. Arar, "Renewable energy harvesting for wireless sensor networks in precision agriculture", *International Journal of Networked and Distributed Computing*, vol. 12, pp. 8–16, 2024. DOI: 10.1007/s44227-023-00017-6.

[6] O. Kanoun *et al.*, "Energy-aware system design for autonomous wireless sensor nodes: A comprehensive review", *Sensors*, vol. 21, no. 2, 2021. DOI: 10.3390/s21020548.

[7] M. Prauzek, J. Konecny, and T. Paterova, "An analysis of double *Q*-learning-based energy management strategies for TEG-powered IoT devices", *IEEE Internet of Things Journal*, vol. 10, no. 21, pp. 18919–18929, 2023. DOI: 10.1109/JIOT.2023.3283599.

[8] P. B. Leelavinodhan, M. Vecchio, F. Antonelli, A. Maestrini, and D. Brunelli, "Design and implementation of an energy-efficient weather station for wind data collection", *Sensors*, vol. 21, no. 11, p. 3831, 2021. DOI: 10.3390/s21113831.

[9] H. Cai, W. Qin, L. Wang, B. Hu, and M. Zhang, "Hourly clear-sky solar irradiance estimation in China: Model review and validations", *Solar Energy*, vol. 226, pp. 468–482, 2021. DOI: 10.1016/j.solener.2021.08.066.

[10] H. C. Hottel, "A simple model for estimating the transmittance of direct solar radiation through clear atmospheres", *Solar Energy*, vol. 18, no. 2, pp. 129–134, 1976. DOI: 10.1016/0038-092X(76)90045-1.

[11] H. D. Kambezidis, K. Mimidis, and K. A. Kavadias, "The solar energy potential of Greece for flat-plate solar panels mounted on double-axis systems", *Energies*, vol. 16, no. 13, p. 5067, 2023. DOI: 10.3390/en16135067.

[12] J. A. Ruiz-Arias, "SPARTA: Solar parameterization for the radiative transfer of the cloudless atmosphere", *Renewable and Sustainable Energy Reviews*, vol. 188, art. 113833, 2023. DOI: 10.1016/j.rser.2023.113833.

[13] Y. Dazhi, P. Jirutitijaroen, and W. M. Walsh, "Hourly solar irradiance time series forecasting using cloud cover index", *Solar Energy*, vol. 86, no. 12, pp. 3531–3543, 2012. DOI: 10.1016/j.solener.2012.07.029.

[14] F. J. Diez, A. Martínez-Rodríguez, L. M. Navas-Gracia, L. Chico-Santamarta, A. Correa-Guimaraes, and R. Andara, "Estimation of the hourly global solar irradiation on the tilted and oriented plane of photovoltaic solar panels applied to greenhouse production", *Agronomy*, vol. 11, no. 3, p. 495, 2021. DOI: 10.3390/agronomy11030495.

[15] C. Furlan, A. P. de Oliveira, J. Soares, G. Codato, and J. F. Escobedo, "The role of clouds in improving the regression model for hourly values of diffuse solar radiation", *Applied Energy*, vol. 92, pp. 240–254, 2012. DOI: 10.1016/j.apenergy.2011.10.032.

[16] Solar calculation details. [Online]. Available: https://gml.noaa.gov/grad/solcalc/calcdetails.html

[17] F. Kasten and A. T. Young, "Revised optical air mass tables and approximation formula", *Applied Optics*, vol. 28, no. 22, pp. 4735–4738, 1989. DOI: 10.1364/AO.28.004735.

[18] Solarmodel. [Online]. Available: https://github.com/CHO0178/SolarModel